EFDA–JET–CP(13)03/31

S. Marsen, L. Aho-Mantila, S. Brezinsek, T. Eich, C. Giroud, M. Groth,
S. Jachmich, B. Sieglin
and JET EFDA contributors

# Divertor Heat Load in JET - Comparing Langmuir Probe and IR Data

# Divertor Heat Load in JET - Comparing Langmuir Probe and IR Data

S. Marsen[1], L. Aho-Mantila[2], S. Brezinsek[3], T. Eich[4], C. Giroud[5], M. Groth[6], S. Jachmich[7], B. Sieglin[4] and JET EFDA contributors*

***JET-EFDA, Culham Science Centre, OX14 3DB, Abingdon, UK***

*[1]Max-Planck-Institut für Plasmaphysik, EURATOM-Assoziation, 17491 Greifswald, Germany*
*[2]VTT Technical Research Centre of Finland, Association EURATOM-Tekes, FIN-02044 VTT, Finland*
*[3]FZ Jülich, Institute of Energy Research - Plasma Physics, EURATOM Association, Jülich, Germany*
*[4]Max-Planck-Institut für Plasmaphysik, EURATOM-Assoziation, 85748 Garching, Germany*
*[5]EURATOM-CCFE Fusion Association, Culham Science Centre, OX14 3DB, Abingdon, OXON, UK*
*[6]Aalto University, Association EURATOM-Tekes, P.O.Box 14100, FIN-00076 Aalto, Finland*
*[7]Laboratory for Plasma Physics, ERM/KMS, Assoziation EURATOM Etat Belge, Brussels, Belgium*

Preprint of Paper to be submitted for publication in Proceedings of the
40th EPS Conference on Plasma Physics, Espoo, Finland.
1st July 2013 – 5th July 2013

The heat flux to the target plates $q_p$ is a crucial design parameter for fusion machines. In attached regimes the majority of the power entering the SOL across the separatrix flows to a narrow region on the divertor target plates. Predictions of heat loads in future machines are typically based on scaling laws derived from experimental data. $q_p$ can be measured by infrared (IR) cameras viewing the target plates. Alternatively, Langmuir probes can be used to determine qp from the temperature and particle flux measured at the sheath edge in close proximity to the target plates (<<1mm). Measuring $q_p$ with probes involves physics of the sheath in which energy is transferred from electrons to ions. Relating $q_p$ to the electron temperature $T_e$ and the particle flux $\Gamma$ at the sheath edge leads to the definition of the sheath heat transmission coefficient $\gamma = q_p = T_e\Gamma$. $\gamma$ can be expressed in terms of plasma parameters [1, 2]:

$$\gamma = \left( 2.5\frac{T_i}{T_e} - ln\left( \sqrt{2\pi \frac{m_e}{m_i}\left(1+\frac{T_i}{T_e}\right)}\frac{1-j_0/j_s}{1-\delta}\right)\right) + \frac{2(1-j_0/j_s)}{1-\delta} + \varepsilon_{pre} + \frac{\chi_i}{kT_e} + \frac{\chi_r}{kT_e} \qquad (1)$$

$\varepsilon_{pre} \approx 0.5$ is related to pre-shaeth acceleration of ions, $\chi_i$ is electron-ion and $\chi_r$ atom-atom recombination energy. $T_i$ is the ion temperature, $m_{e;i}$ the electron and ion mass, respectively. Divertor targets are typically not floating but electrically connected to the vessel. Thus, they can draw a net current $j_0$ which alters $\gamma$ compared to a floating target. $j_s$ is the ion saturation current which equals the particle flux to a floating target. Secondary electron emission ($\delta$) and reflections of particles and energy can affect $\gamma$ and depend on the target material. However, they are neglected in our analysis since they are expected to be very small for shallow field line impact angles and it was shown experimentally in JET that the target material has no measurable impact on $\gamma$ [3]. Therefore we show data from JET equipped with a carbon divertor and with tungsten as target material.

$\gamma$ can be derived experimentally by comparing IR and probe data. Reasonable agreement between sheath theory and experiments is typically found in sheath limited regimes with low recycling. But with increasing density they deviate significantly which is typically attributed to an overestimation of plasma parameters by probes.

In JET, the target heat flux is measured by IR thermography with a spatial resolution of 1.7mm. Target probe arrays are installed at 3 toroidal positions with probes at 35 poloidal positions each. They can be configured as triple probes or individually swept single probes. Figure1 shows the probe design on the outer horizontal target. The probes are wedge shaped with an inclination of 13° in order to get a well defined collecting area as compared to flush mounted probes which suffer from extremely shallow field line impact. Regular ohmic monitoring pulses are used to monitor the erosion of the probe tips.

Single probe analysis is based on a least squares fit of an asymmetric double probe characteristic to the data, Eq.2

$$j = -j_s\left(1+\delta a\left(V_{fl}-V_{pr}\right)\right)\frac{1-exp\left(\frac{e\left(-V_{pr}-V_{fl}\right)}{kT_e}\right)}{\alpha + exp\left(\frac{e\left(-V_{pr}-V_{fl}\right)}{kT_e}\right)} \qquad (2)$$

$V_{fl}$ is the floating potential and $V_{pr}$ is the biasing potential of the probe tip. $\alpha$ is the ratio of ion to electron saturation current. The parameter $\delta a$ leads to an effectively increasing probe area with increasing biasing. On the one hand this can be due to an expanding Debye sheath around the probe [4], which is, however, more of an issue to flush mounted probes with effective probe size close to the Debye length. However, finite plasma resistivity can also affect the entire probe circuit causing similar effects on the probe characteristics [5].

L-mode discharges give the best quality data for a comparison of IR and Langmuir probes. Strike point sweeps of ≈ ±2cm on the target are used to create profiles from probe data. At low ($\int ndl 5.4 \cdot 10^{19} m^{-2}$) an excellent agreement of $q_{\mathrm{p}}$ from probes and IR was found as can be seen in Fig.2. $q_{\mathrm{p}}$ from probes in this case was calculated with $\gamma$ derived from Eq.1 using profiles of $T_{\mathrm{e}}$ and $j_0 = j_s$ and assuming $T_i = T_e$.

The resulting profile of $\gamma$ together with an experimental $\gamma_{Exp} = q_{\mathrm{p,IR}} / T_e j_s$ is also shown in Fig.2. The shape of the profile with slightly higher values of $\gamma$ at the peak is related to a net electron current drawn by the grounded divertor tiles. The probe data in this case were analysed enforcing $\delta a = 0$. As shown in Fig.3 the inclusion of a finite $\delta a$ would yield an as good fit of the probe data. However, in this case sheath theory would fail to reproduce the power from IR by probes as shown by the dashed line in Fig.2 (top). The probe bias in this case, i.e. at this $T_e \approx 40eV$, is simply not sufficiently negative for the probe current to saturate, wheter or not $\delta a$ is finite.

Neglecting $\delta a$ is further supported by power balance. Estimated target power in Pulse No: 78647 was $P_{target} = P_{heat} - P_{rad} = 2.1$MW which is in good agreement with the sum of power on inner and outer target measured by probes, $P_{LP;inner} + P_{LP;outer} = 2.2$MW. The situation changes with increasing density. Although the actual target power decreases due to more radiation, probes show increasing power as shown in Fig.4. Up to $\int ndl = 7\ 10^{19}\mathrm{m}^{-2}$ the power balance is fulfilled with $\delta a = 0$. At $\int ndl = 8.4\ 10^{19}\mathrm{m}^{-2}$ the probes overestimate the power by ≈25% which is still a reasonable agreement. However, comparing profiles from probes and IR in this case shows a deviation of more than a factor of two at the peak. Looking at the probe characteristics in Fig.3 taken at this density shows rather clearly a non saturation of the ion current. $T_e$ is here sufficiently low and the inclusion of $\delta a \neq 0$ in the analysis turns out to give a better fit of the probe characteristics, reasonable agreement with $q_p$ from IR and a better power balance.

Going to high recycling regimes at further increased density the power from the probes is significantly overestimated. In this case the probe current saturates and $\delta a$ cannot fix the power balance. Deriving $\gamma_{Exp}$ from the direct comparison with IR would yield values as low as $\gamma_{Exp} \approx 2$, which is not compatible with sheat theory. Assuming the probes to measure $j_s$ reliably in this regime puts the root cause on $T_e$ to be overestimated. It was shown before for JET that, with this in mind, one can estimate the true $T_e$ from qp;IR and js by assuming a certain value of $\gamma$ [3]. On the other hand it is argued in literature that this is a regime in which the probes overestimate js. This is because with the probe bias, electron heat flux to the probe surface is reduced. Thus, the local electron temperature is raised, enhancing neutral ionization and increasing the ion flux to the probe [6].

It is not within the scope of this paper to resolve this issue. However, since probe data analysis is well known to be a delicate topic, it turns out that comparison with heat flux from IR thermography and a global power balance are a good measure for data validation. Fig.5 shows an application of this exercise in L-mode experiments with $N_2$ seeding in the divertor.

The power to the target is expected to decrease due to increasing radiation. This is confirmed by probe measurements. However, neglecting $\delta\alpha$ in the analysis would suggest the power to increase up to intermediate $N_2$ levels and finally to decrease. This is mainly due to an overestimation of $q_p$ on the inner target at intermediate levels.

## REFERENCES


[1]. P. C. Stangeby, The Plasma Boundary of Magnetic Fusion Devices, IoP publishing, (2000)

[2]. D. Brunner et al., Review of Scientific Instruments, **83**, 033501 (2012)

[3]. S. Marsen et al., Journal of Nuclear Materials, **438**, Suppl., S393 - S396 (2013)

[4]. J. P. Gunn et al., Review of Scientific Instruments, **66**, 154-159 (1995)

[5]. P. C. Stangeby et al., Plasma Physics and Controlled Fusion, **37**, 1337 (1995)

[6]. D. Brunner et al., Journal of Nuclear Materials, **438**, Suppl., S1196 - S1199 (2013)


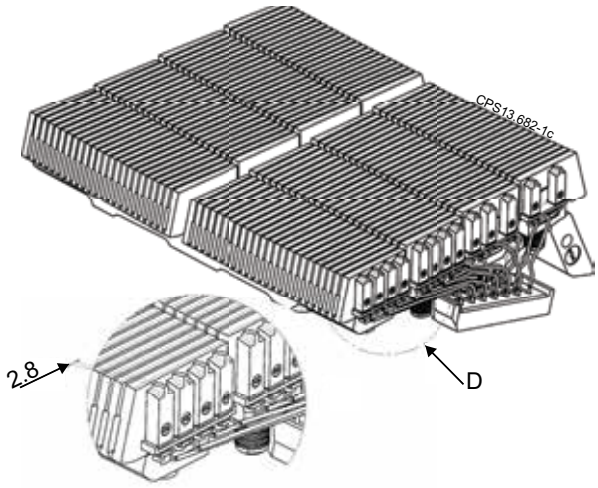


*Figure 1: Design of the JET divertor Langmuir probes. Wedge shaped probes are attached to the target tiles.*

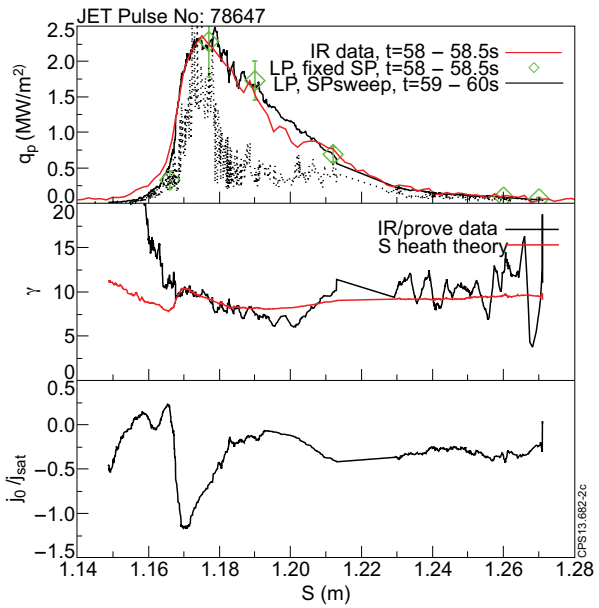


*Figure 2: top: Target heat flux ($q_p$) on outer target at low density. IR data (red) compared to probe data (black). $\delta a$ = 0 was enforced for the solid line. Dashed is with $\delta a$ as free fit parameter. middle: $\gamma$ from direct IR-probe comparison (black) and from sheath theory (red). bottom: Ratio of probe current at 0V and ion saturation current.*

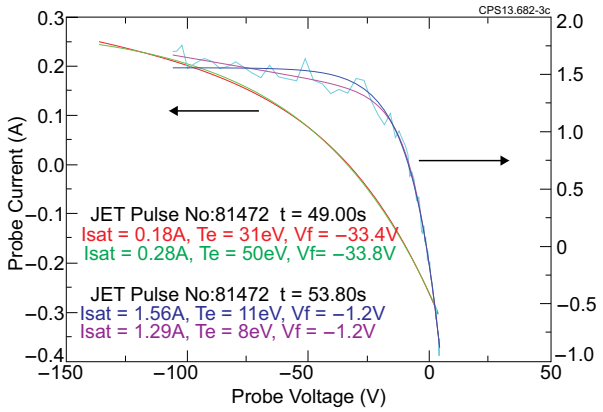


*Figure 3: Probe characteristics measured at ∫ndl = 5.6 $10^{19}m^{-2}$ R (black) and ∫ndl = 8.4 $10^{19}m^{-2}$ (cyan). red and blue are corresponding fitted characteristics enforcing δa = 0. green and magenta with δa ≠ 0 (solid)*

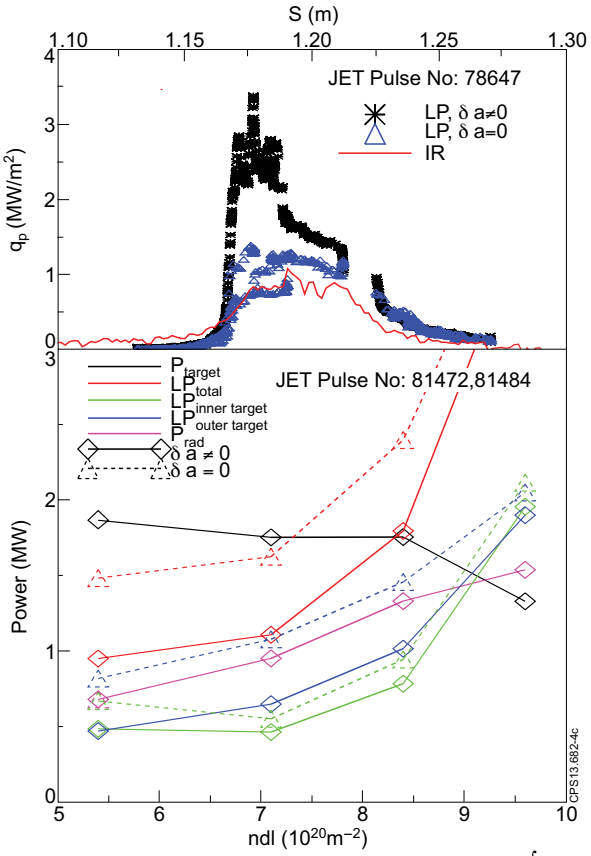


*Figure 4: Top - Profiles of $q_p$ on the outer target at ∫ndl = 8.4 $10^{19}m^{-2}$. Bottom - Power balance during a density scan comparing probe analysis with δa = 0 (dashed) and δa ≠ 0 (solid).*

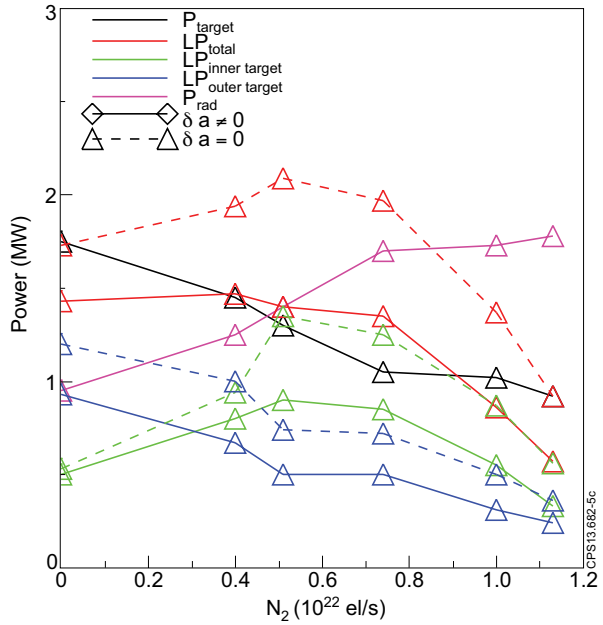


*Figure 5: Power balance from Langmuir probes during $N_2$ seeding in L-mode.*